Computer Fraud and Security
ISSN (online): 1873-7056

Numerical Investigation of Concrete and Helical Pile-Supported Embankments Under Railway Traffic Loading

Dongmei Chen[1],Yueshun Chen [2*] , Haisu Zhao[3]

1. Wuhan Railway Vocational College of Technology, School of Railway Engineering, Wuhan, Hubei Province, China, 430205

2. Hubei University of Technology , School of Civil Engineering Architecture & the environment,

Hubei Wuhan , China, 430068

3.China Railway Siyuan Group Engineering Operation and Maintenance Co., Ltd., Hubei Wuhan , China, 430205

Corresponding Author：Yueshun Chen, yueshunchen@163.com

Abstract

Pile structures increase embankment stability and settlement control. Recent research has focused on helical piles' enhanced compressive and tensile performance, rapid installation, and absence of concrete problems. This numerical study compares helical and concrete pile-supported embankments. A three-dimensional finite element model was developed using ABAQUS software to evaluate soft soil embankments with equal pile length and diameter. The numerical model was verified by field and lab measurements. Helical piles decrease embankment, soft soil settling, and control lateral displacement better than concrete piles. Furthermore, the distribution of axial forces along the embedded depth demonstrates that helical piles exhibit higher bearing capacity and function in a frictional manner. The inclusion of a pile cap was also examined, revealing that it enhances load distribution, reduces vertical settlement by 19%, and improves stress transfer efficiency. However, adding additional helical blades to the pile body does not significantly improve embankment performance and primarily affects the load transfer mechanism at specific spacing ratios.

Keywords: Pile-supported embankment, Helical piles, Concrete piles, Bearing capacity, Numerical modeling, Railway traffic loading, Settlement control, Load transfer mechanism

Introduction

Construction of embankments on soft clay soils is challenging for geotechnical engineers due to their low bearing capacity, high settlement, and instability of the embankment slope. Various methods have been used to improve the engineering properties of these types of soils. Pile-supported embankments are more commonly used due to their fast and cheap construction and reduced total and differential settlements compared to other traditional methods of improving soft soils [1-5]. Various studies have been conducted on pile-supported embankments and the factors affecting their performance under various static and dynamic loads. Most of the studies have focused on using concrete piles, which are in situ or prefabricated [6-8] and presented an extensive parametric study using 3D numerical modelling on pile-reinforced and geosynthetic-reinforced embankments. Numerical analysis was performed on cohesive and noncohesive embankments to emphasize the influence of soil cohesion on the performance of the embankment in load transfer and settlement [9-12]. A study was conducted on the performance of concrete pile-supported embankments under railway traffic loads; this study studied the elastic modulus of the pile and the embankment, the angle of internal friction of the embankment materials, and the pile spacing. The effects on pile-supported embankment performance were explored. Article [13] conducted a field study of a pile-supported embankment system. The embankment was constructed with a height of 40 m on prestressed concrete piles. A series of field tests, including pile head loading, settlement and lateral displacements, were carried out. In [14], by

numerically investigating the performance of embankments supported by end-loaded and friction piles, it showed that the use of friction piles can significantly reduce settlement and found that the embankment load transferred from the pile to the foundation soil depends significantly on the pile length. Article [15] presents a numerical analysis of a slab-pile-supported embankment for China's Beijing Tianjin high-speed railway. (Cement-fly ash- gravel) (CFG) piles were used in this project, and the results were compared with field data. The results show that the CFG columns carried most of the embankment load. Combining rigid piles and reinforced concrete slabs significantly reduced the vertical stresses applied to the soil between the piles [16-19]. Moreover, [20] studied the full-scale performance of pile-supported embankments in field projects. The results show that using piles can reduce the pressure exerted on the soft soil beneath the embankment and allow a more significant share of the load to be transferred to the piles. Previous research implies pile-supported embankment screw piles require further study. A screw pile is a deep foundation system made of steel and consists of one or more connected helical bearing plates connected at various intervals along a central shaft. Figure (1) shows an example of a screw pile with two helices. The shaft diameter (D) is usually between 178 mm and 914 mm, and the blade diameter (DP) is usually 2 to 3 times the diameter of the helical plate [21-25]. The use of screw piles has made significant progress in engineering applications in recent years due to their high bearing capacity for compressive loads. A screw pile can be driven into the ground at any depth and any angle (depending on soil conditions) by the axial force and torque applied to the top of the pile by a hydraulic torque motor. The advantages of using screw piles over concrete piles include:

- Ability to be removed and reinstalled.
- Reduced drilling hazards and eliminated the problem of pouring concrete.
- Low noise, minimal vibration and more excellent environmental compatibility.
- No waste during drilling and reusability.
- Use in a wide range of soils [26-29].

Various researchers have studied the performance of screw piles. Article [30] studied the axial compression behaviour of screw piles in sand and clay. They proposed a method for designing screw piles using the results of numerical models. In [31] also compared the performance of screw piles with concrete piles under lateral and axial loads.

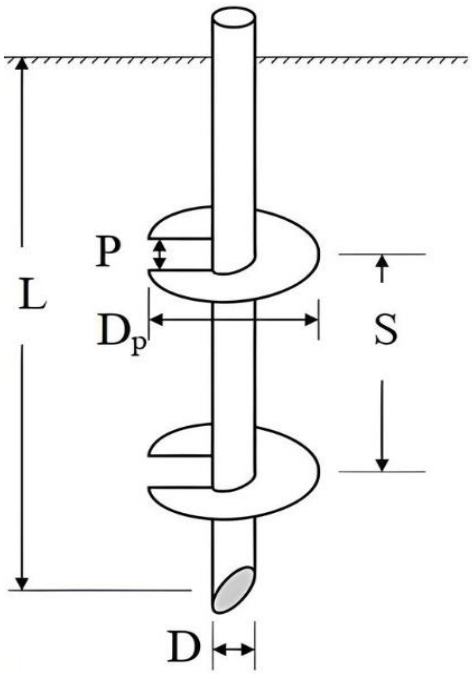

Figure 1: Example of a double-bladed screw pile

A review of the technical literature shows that the behavior of civil embankments with screw piles requires further study. Given the aforementioned advantages, screw piles can be considered a suitable alternative to concrete piles. In this study, assuming the same geotechnical characteristics of the soil and loading conditions, the performance of screw and concrete piles is compared, and the load transfer mechanism in the embankment, as well as the amount of vertical and horizontal settlements and displacements of the embankment, is investigated. Finally, the pile cap and its effects on the performance of screw piles and the reduction of horizontal and vertical settlements of the embankment are studied.

Numerical modeling

In order to build the pile-supported embankment model studied in this paper, the finite element software Abaqus was used. In order to accurately examine the studies performed, the models created were in three dimensions, and due to the symmetry of the model, only half of the model was built.

Model geometry

This study models a 1.5:1 embankment with a 6 m height and 7.5 m crest length. The embankment was constructed on a uniform layer of soft clay soil with a height of 30 m. The dimensions of the foundation soil were extended to a length of 70 m to provide boundary conditions and reduce its effect on the structure's displacement stress and strain fields. The perpendicular dimension to the plane was four due to using a single row of piles [32]. Hollow shaft screw piles and solid concrete piles with a cap measuring 1.5 x 0.5 x 1.5 m were used. In this study, the pile lengths were assumed to be equal. The shaft diameter of the screw pile was assumed to be the same as that of the solid concrete pile by the study [31]. Figure (2) shows the dimensions of the three piles and the embankment modeled in this paper.

The geometric specifications of the piles are also summarized in Table (1). The modeling process can be explained as follows: In the first step of the analysis, in situ, stresses are introduced into the soil using the geostatic step, and then the piles are placed in the soil, and the displacements and stresses created are equal to zero. In the next step, an embankment with a height of 6 meters is loaded in 3 stages with dimensions of 2 meters under the weight of the embankment soil, and then in the last step, the equivalent traffic loading stress is applied to the embankment crest.

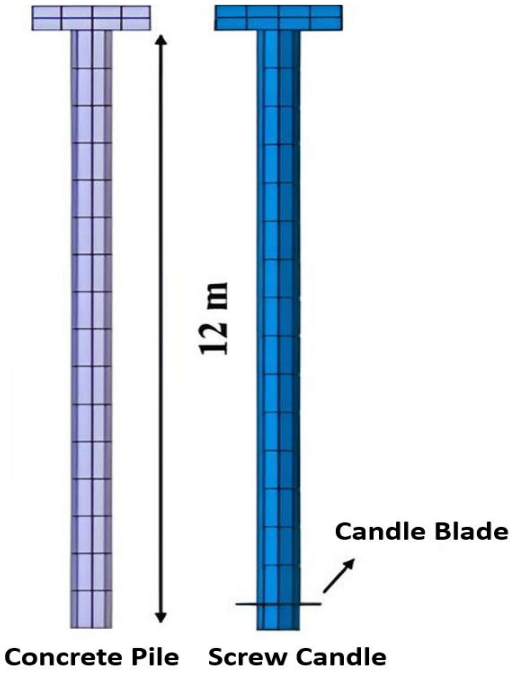

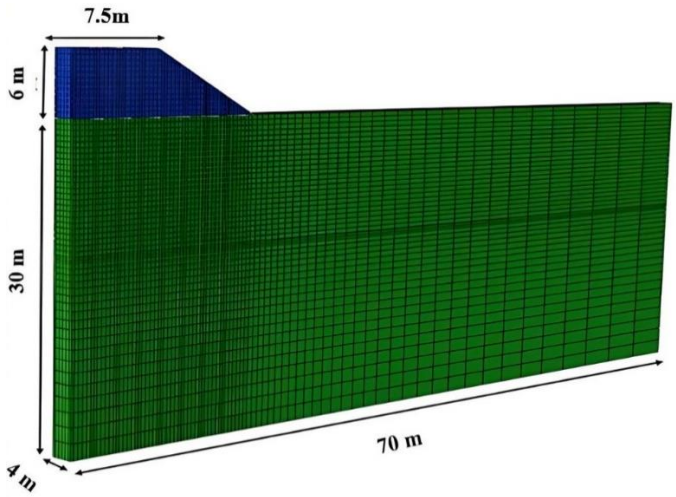

Figure 2: Finite element model meshing and dimensions used in the model

Table 1: Geometric parameters of piles used in the finite element model

Geometrical specifications	Screw pile	Concrete pile
Pile length (m)	12	12
Shaft diameter (m)	0.05	0.05
Shaft thickness (m)	0.01	-
Spiral diameter (m)	1	-
Spiral thickness (m)	0.025	-

Material parameters and behavioral model

The embankment material is generally made of granular soils, which are considered dry in this study. Also, the foundation soil is made of soft clay soil with poor geotechnical properties. Drainage is assumed to have occurred for clay soil, and drainage parameters are used for the soil. Different engineering properties for soils have been reported in different papers. The parameters and dimensions assumed for piles and soil in this study have been selected from the papers mentioned in the research records. The mechanical and geotechnical parameters used for soil and piles in this study are generally stated in Table (2). The Mohr-Coulomb elastoplastic behavior model was used to model granular and clay soils, and the concrete and screw piles were modeled as linear elastic. The tangential behavior of the soil-pile interface was defined using the Coulomb friction model of the penalty type, in which the relative tangential motion is zero until the shear stress reaches a critical value. When the shear stress exceeds the shear strength of the contact surface or the contact surface pressure, slippage occurs. The interaction coefficient between the soil and the pile in this study is 0.7 [33, 34].

Table 2: Finite element model material parameters

Material	E(MPa)	$\gamma\left(\frac{kN}{m^3}\right)$	φ′	ν	C(KPa)
Embankment	15	20	30 0.3	30 0.3	5
Soft soil	5	18.4	22 0.3	22 0.3	8
Concrete	35000	2400	-	0.2	-
Steel	210000	7850	-	0.15	-

Gridding and Boundary Conditions

Figure (2) shows the gridded view of the pile-supported embankment in the finite element model. The element size around the pile and the soil and embankment's contact surface are considered finer. 8-node elements with reduced integration (C3D8R) are used to model the pile and soil. In order to reduce the effect of the boundary conditions on the results, the model boundaries are extended. Model boundary conditions set the bottom boundary three-direction displacements (UX=UY=UZ=0) to zero. The x and y displacements on both sides of the model are also zero (UX=0, UY=0).

Traffic loading simulation

The effect of the structure's stress-strain state under train traffic load is applied as a vertical overhead load evenly distributed across the sleeper width. For loading simulation, the LM71 train model shown in Figure (3) was used by publication 279 of the Technical and General Specifications for Railway Infrastructure [35-37].

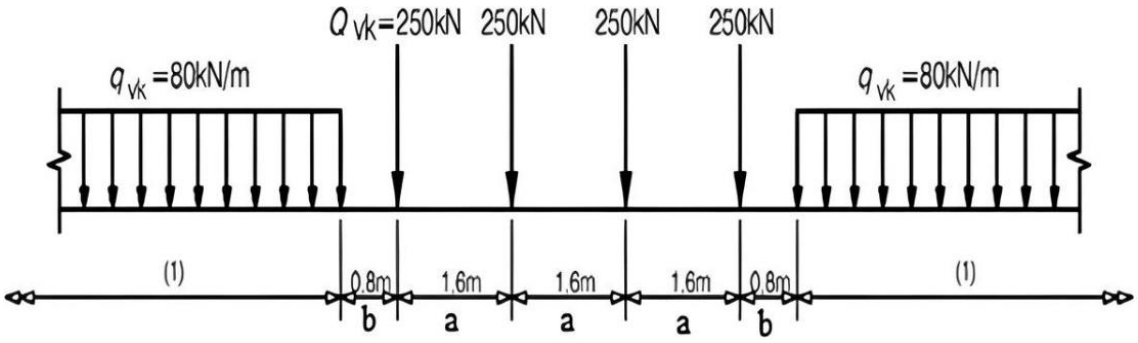

Figure 3: LM71 train loading model

In order to distribute the stress uniformly across the crosspiece, the following equation was used to convert the wheel axial load into a uniform extended load, taking into account the LM71 loading values:

$$q = \frac{4 \times Q_{vk}}{(3 \times a + 2 \times b) \times B} \quad (1)$$

According to the Figure (3), Q_{vk} is the concentrated load of 250 kN. Also, the parameters a and b are geometric, the values of which are 1.6 and 0.8 m, respectively, according to publication 279. Also, B is the parameter indicating the loading width. In this problem, the value of B is taken as 2.5 m, equivalent to a sleeper's standard length. It is the dynamic impact coefficient for which various empirical relations have been reported. For the effect of the dynamic effects of railway loading, the spread load obtained from relation (1) is multiplied by the value α. In this study, the American Railway Engineering Association (AREA) standard was used, the relationship of which is as follows:

$$\alpha = 1 + \frac{0.00521 + V}{D_w} \quad (2)$$

In equation (2), Dw is the wheel diameter, 1 m, and V (km/h) is the train speed, which is assumed to be 160 in this study.

Validation of numerical modeling

In this section, two models are selected for validation of numerical modeling based on the reported field data of the pile-supported embankment and the laboratory data related to the loading of a screw pile tested in actual dimensions.

Pile-supported embankment

In order to verify the modeling and the results of the numerical analyses, the data reported from a field project of a pile-supported embankment system by [20] were used. Tables (3) and (4) show the validation model's soil properties and pile geometry, respectively. The numerical model of the embankment was developed with the finite element software Abaqus, and the numerical results were compared with those reported from the field data. Figure (4) shows the dimensions of the embankment and piles and their location. Comparison of the results shows a good agreement between the numerical model results and the field data. Figure (5) shows the settlement rate at the pile cap, and Figure (6) shows the settlement rate at the soft soil surface between the piles compared to the time of embankment construction. Considering that the embankment was constructed over 65 days, a break in the trend of the above graphs is observed shortly after the end of this time.

Table 3: Soil parameters used in validation models

Pile embankment					
Material	**E (MPa)**	**$\gamma(\frac{kN}{m3})$**	**φ'**	**v**	**C (KPa)**
Embankment	21	15	32	0.3	0
ML	6.5	19.3	21	0.35	0
CL	2.4	16.7	24	0.3	0
GM	40	19.4	30	0.27	0
Helical pile					
Depth (m)	**E (MPa)**	**$\gamma(\frac{kN}{m3})$**	**φ'**	**v**	**Ψ**
0-5	50	20	24	0.3	10
5-9	50	20	21	0.3	10

Table 4: Geometric characteristics of piles used in validation models

Parameter	**Helical pile**	**Pile embankment**
Shaft diameter (mm)	273	400
Depth of pile (m)	5.5	20
Helix diameter (mm)	610	-
Number of helix	1	-

Thickness of the shaft (mm)	9.3	50
Thickness of the helix (mm)	20	-

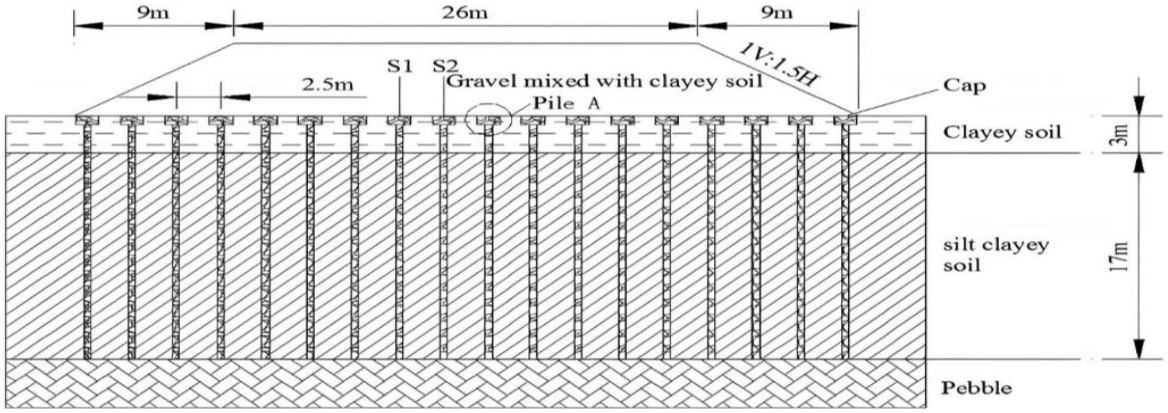

Figure 4: Cross section of the TJ highway embankment

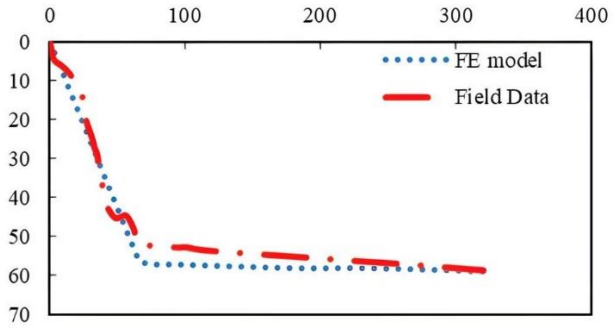

Figure 5: Pile cap settlement versus time

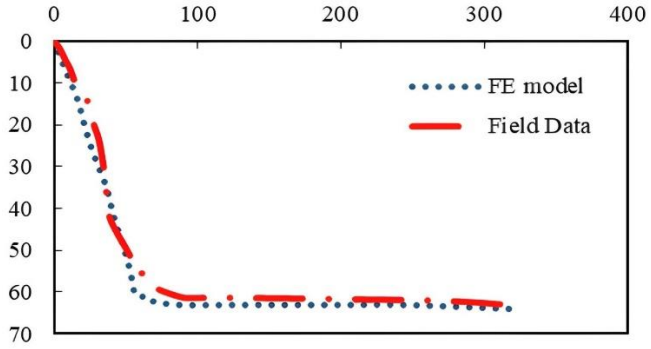

Figure 6: Soil surface settlement versus time

Screw pile

Also, to ensure the correct way of modeling the screw pile, a screw pile example (Site A - PA1) reported by [30] was modeled by Abacus software. Most of the numerical studies conducted have been modeled as a cylindrical disk. The reason why an ideal spiral modeling the soil properties and the modeled screw pile are listed in Tables (3) and (4),

respectively. The screw pile spiral is not included in the model to enable modeling under axial symmetry conditions and to reduce the complexity of the model in construction and meshing [22]. The pile settlement load diagram in Figure (7) has been shown.

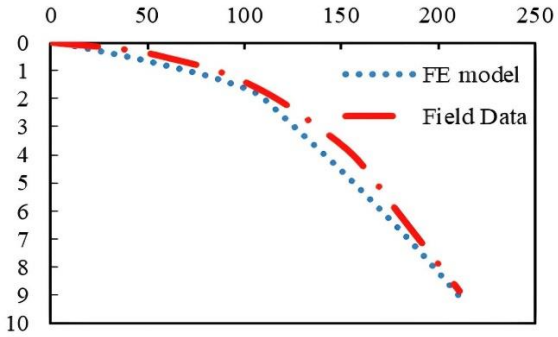

Figure 7: Comparison of numerical model results with field data from the PA-1 experiment

Discussion and analysis of finite element results

In this section, the vertical and horizontal displacements in an embankment system based on screw and concrete piles are investigated. The axial force distribution along the buried depth of screw and concrete piles is compared. The load transfer mechanism between these two piles is compared by defining the stress reduction ratio parameter. The effect of the cap on the screw pile is also studied.

Comparison of the performance of concrete and screw piles

A group of concrete and screw piles in a pile-based embankment is studied. The piles are modeled at 2-meter intervals, and all soil parameters and dimensions are assumed to be the same in the model, and only the pile type is changed. Also, a uniform stress of 115 kN/m2 is distributed over the embankment surface for modeling the railway load. Figure (8) shows axial force distribution along the screw and concrete piles' buried depth at the embankment center. Figure (8) shows that screw piles have a better bearing capacity at the pile head and wall than concrete piles, enhancing the embankment system. Because the screw pile has a reduced cross-sectional area, the concrete pile top has a larger bearing capacity. Pile frictional behavior decreases embankment and soil settlements less than pile wall capacity.

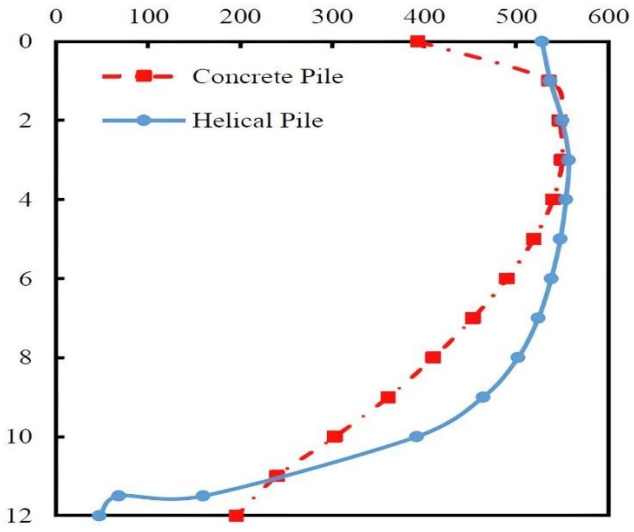

Figure 8: Axial force distribution along pile depth

The settlement rate at the base soil surface is shown in Figure (9); the results show that screw piles have a more effective performance in controlling the settlement rate at the base soil surface compared to solid concrete piles. The maximum settlement rate is for the center of the embankment supported by the pile, and with increasing distance from the center of the model, both the settlement rate of the base soil decreases. The settlement difference between concrete and screw piles decreases, which can be concluded that by reducing the stress caused by the weight of the soil and traffic loading, the difference in performance between screw and concrete piles also decreases. The horizontal and vertical settlements of the granular embankment are also compared in explaining the performance of concrete and screw piles. Figure (10) shows the contour of vertical settlement changes, and Figure (11) shows the contour of horizontal displacement changes in the granular embankment. The highest vertical settlement in the embankment occurred under traffic load, and the lowest value occurred at the toe of the embankment. The results show that the screw pile has a better performance in controlling the settlement rate along the embankment, so the highest settlement for the embankment with concrete pile is 39 cm, and for the screw pile, this value reaches about 35 cm. In comparing the horizontal displacement contours in the embankment, the screw piles also have a positive performance compared to the concrete piles so that a smaller failure wedge is formed at the top of the slope of the embankment supported by the screw pile compared to the embankment supported by the concrete pile.

Soil Arching Ratio defines pile-supported embankment load transmission. This ratio is a numerical value between 0 and 1, where SAR=0 indicates that the load transfer mechanism has occurred entirely, and SAR=1 indicates that the load transfer mechanism has not occurred. The entire load of the embankment is transferred to the soil below the embankment [38]:

$$\mathrm{SAR} = \frac{\sigma_s}{\gamma_e \mathrm{H} + \mathrm{q}} \tag{3}$$

In equation (3), the spread load is considered uniformly over the entire embankment surface; in this paper, because the simulated traffic load is applied to a section of the embankment and is not applied uniformly along the embankment crest, it has been neglected and only the weight of the embankment layers has been considered.

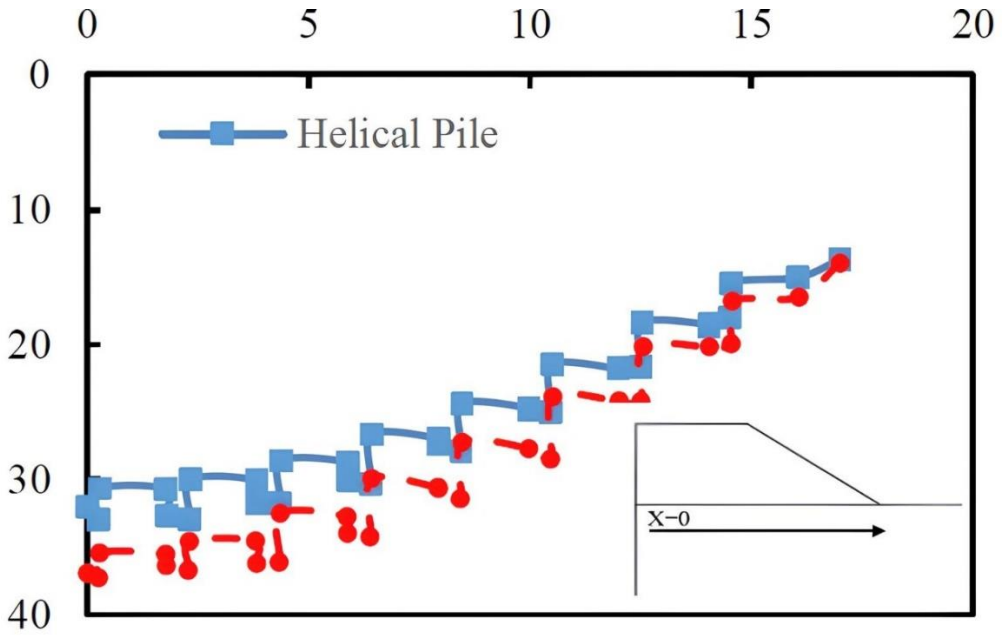

Figure 9: Soil settlement under the embankment from the center of the embankment to the end of the embankment

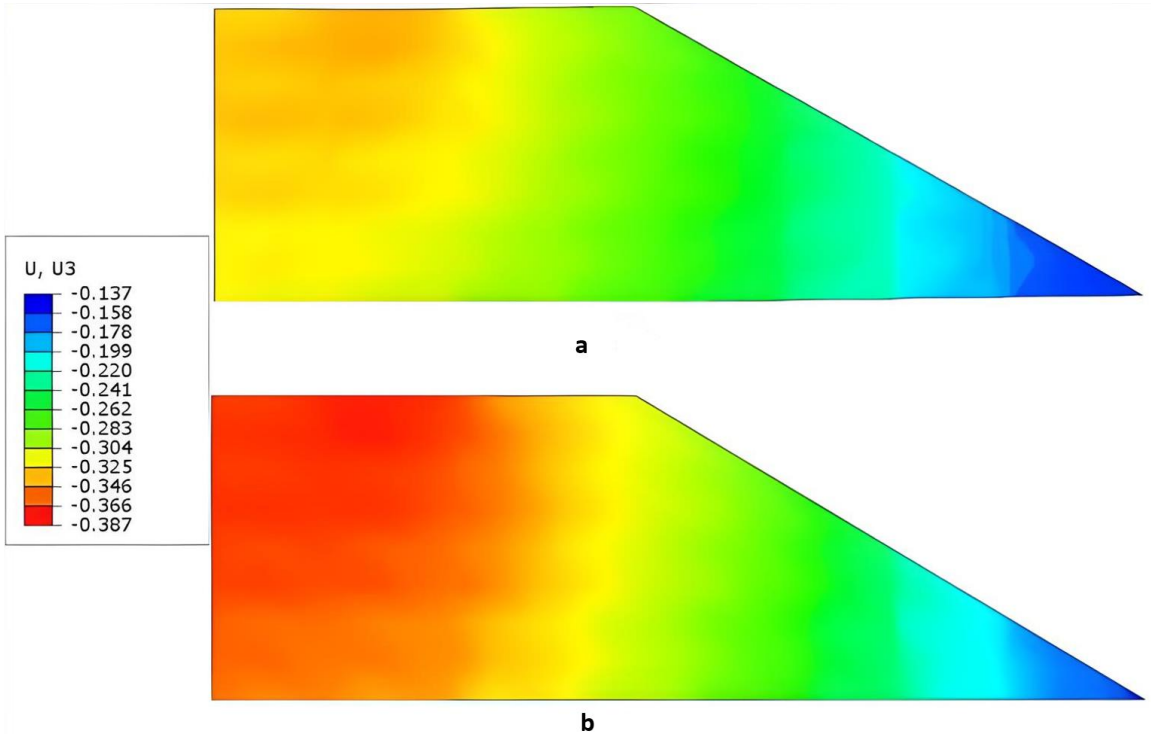

Figure 10: Vertical displacement contour of granular embankment: (a) screw pile, (b) concrete pile

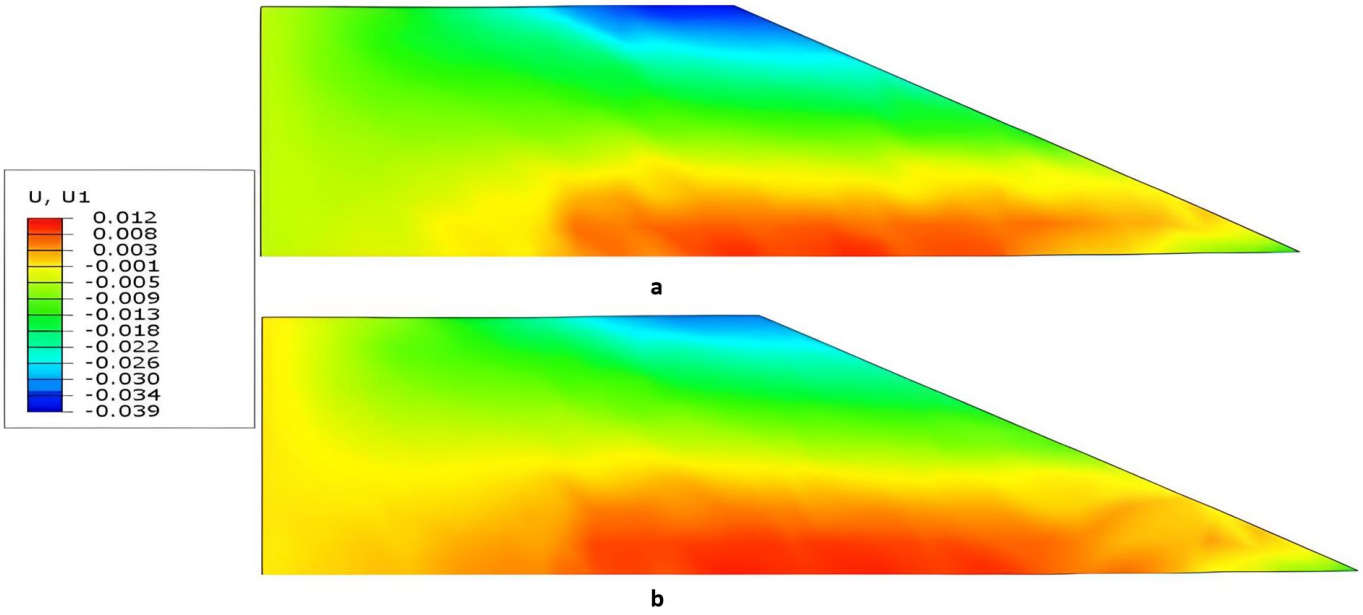

Figure 11: Horizontal displacement contour of fine-grained soil: (a) concrete pile, (b) screw pile

Figure (12) shows the stress reduction ratio for concrete and screw piles, taking into account the effect of the loading intensity due to the weight of the embankment. The results show that concrete piles have a higher efficiency than screw piles, contrary to the results of the previous page showing that screw piles have a significant performance in controlling settlements. The reason for this could be due to the larger cross-sectional area of solid concrete piles compared to screw piles, which allows for a more uniform distribution of stress over the surface of the foundation

soil. Arching phenomena, embankment load transfer to the piles, and foundation soil surface pressure reduction do not immediately reduce settlement in a pile-based embankment system. The results of Figure (12) show that the stress reduction ratio in the system increases with increasing embankment height. This phenomenon occurs because the weight of the embankment does not create sufficient shear resistance for arching at lower embankment heights. The pressure from the foundation soil between the piles decreases, so with increasing embankment height, the applied stress increases, and sufficient shear resistance is formed to create arching and complete the load transfer mechanism. The difference in the graphs also indicates that as embankment increases, the degree of arching eventually reaches a threshold value, and its effect decreases. Another important point is that with the increase in the amount of arching, the difference in the amount of load on the screw and concrete piles also increases, such that this difference is 4 percent at 1.5 meters of embankment and 27 percent at the end of the embankment at a height of 6 meters.

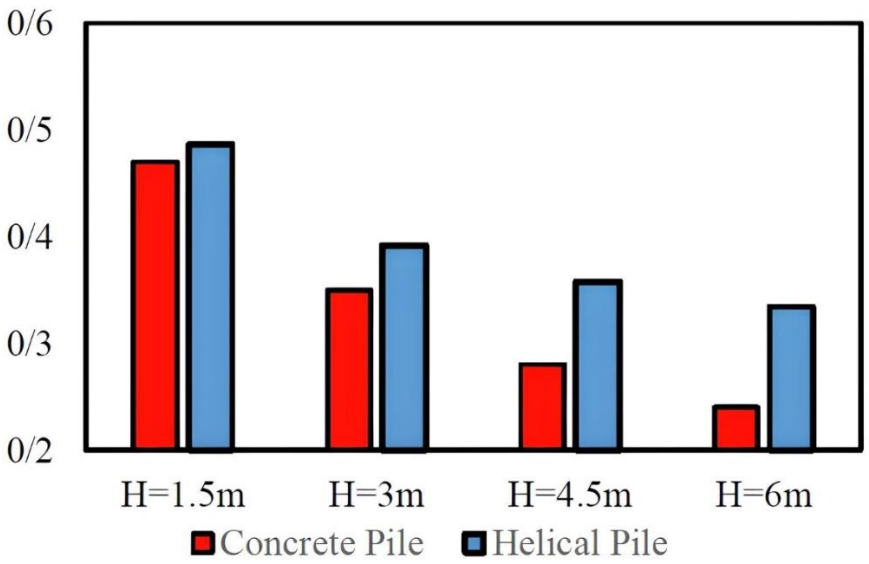

Figure 12: Comparison of stress reduction ratio according to pile type

Comparison of the performance of screw piles with and without caps

In this section, the effect of the cap on an embankment system based on screw piles is studied, the pile dimensions are considered the same, and all modeling and loading conditions and soil parameters are assumed to be the same. Figure (13) shows the difference in axial force distribution along the pile. It is observed that the concrete cap causes better transfer of the embankment stress and loading to the pile head. Therefore, the presence of the cap causes a better load transfer mechanism to the pile head, which results in less stress on the foundation soil and leads to better control in reducing settlements and displacements. Also, the results shown in the stress variation contour in the pile in Figure (14) indicate that the pile wall plays a significant role in the pile's bearing capacity compared to the pile's tip and head. In the analysis of Figure (14), it can be added that negative friction occurs in the lower part of the pile due to the more excellent differential settlement that occurs in the case without a cap.

In contrast, a cap bulges stress distribution and reduces increased pile friction. The piling wall's capacity was used more. Optimal pile stress distribution and foundation soil compressive stress lowering affect vertical and horizontal embankment displacements. Figure (15) shows screw pile embankment vertical changes with and without coverings. According to the finite element model, pile caps reduce vertical settling by 8 cm. By moving away from the embankment center and decreasing pile and foundation soil compressive stress; settlement variations will be minimal; therefore, pile row caps are unimportant.

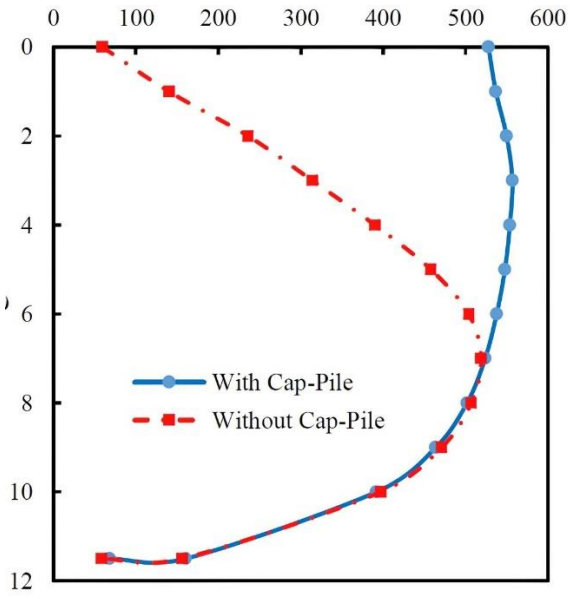

Figure 13: Screw pile axial force distribution along buried depth

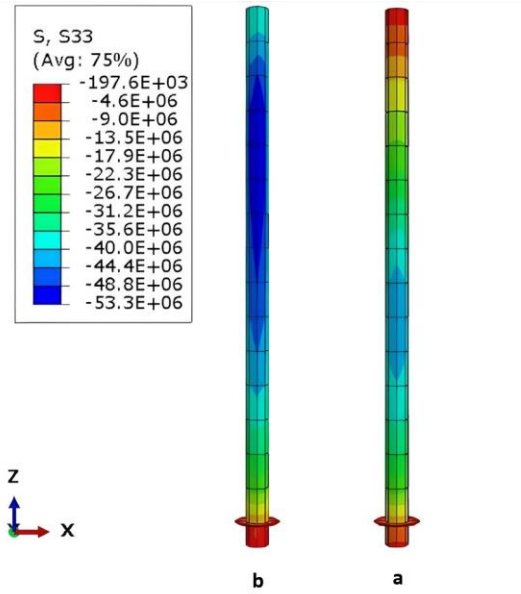

Figure 14: Vertical stress contour of pile shaft wall: (a) pile without cap, (b) pile with cap

Also, in the horizontal deformations shown in Figure (16), the cap has a positive effect, so the horizontal displacement in the embankment toe and the rupture wedge formed at the top of the embankment are smaller. From the results presented, a concrete cap can increase the system's performance and efficiency and significantly reduce the total and differential settlements.

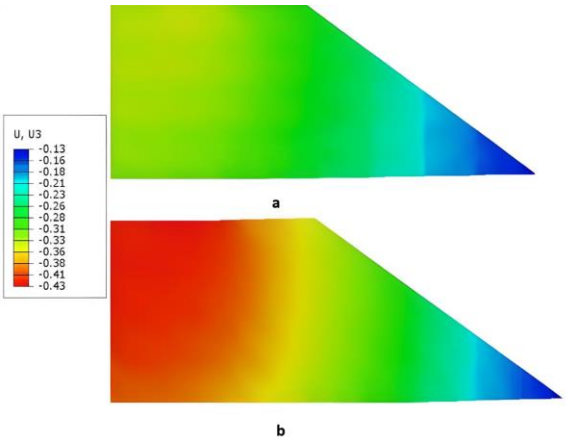

Figure 15: Contour of vertical shape changes of granular embankment: (a) capped pile, (b) uncapped pile

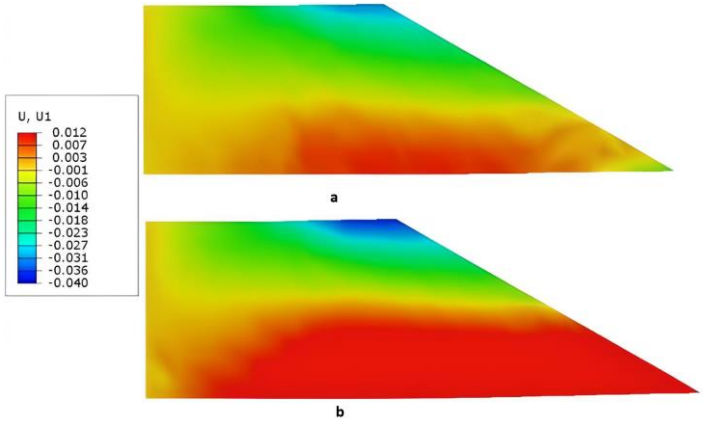

Figure 16: Contour of vertical shape changes of granular embankment: (a) capped pile, (b) uncapped pile

Studying the Effect of Number and Spacing of Blades on the Performance of Screw Pile-Based Embankments

In this section, the effect of the number of blades connected to screw piles with different distances is studied to investigate the load transfer and settlement mechanism in a screw pile-based embankment system. The distance between the screw pile blades is specified by the Spacing Ratio, which is equal to the ratio of the distance between two blades to the blade diameter. Four spacing ratios of 1, 1.5, 2.25, and 3 have been selected for the study, and two cases of 2 and 3 blades connected to the pile body have been assumed for the number of blades. The amount of arching in Figure (17) shows that the number of 2 or 3 blades connected to the pile does not affect the degree of arching of the embankment, and the best case occurs at a distance ratio of 1.5, which is equal to 0.24. With an increase in the distance ratio, the arching ratio increases. With a decrease in this value in the ratio, this value also increases, so it can be concluded that a distance ratio of 1.5 is optimal for controlling the arching ratio in soft clay soils. The arcing ratio in the case of using a single-blade screw pile is 0.32, which is about 25% higher than the 2-blade screw pile with a spacing ratio of 1.5, while it is about 5.88% lower than the 2-blade screw pile with a spacing ratio of 3. The efficiency of the pile head is plotted in Figure (18), and the results show that the highest efficiency occurs at a spacing ratio of 1.5. Also, the results, like the arcing ratio, show the positive performance of the 2-blade screw pile compared to the 3-blade screw pile in all cases. The rate of change in efficiency for the 2-blade screw pile with a spacing ratio of 1.5 is 1.2% higher than that for the single-blade screw pile. Also, the rate of change of a two-blade screw pile compared to a three-blade screw pile with a spacing ratio of 1.5 is 1.2 percent.

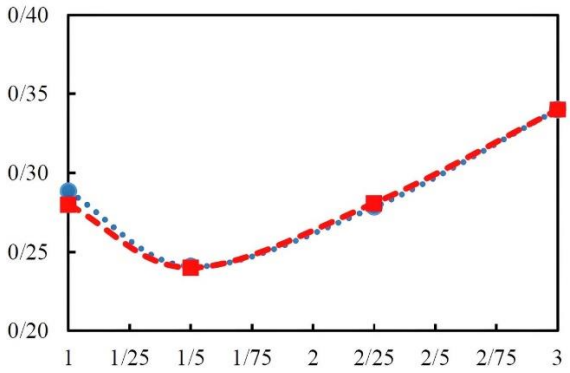

Figure 17: Stress reduction ratio for different spacing ratios in two- and three-blade screw piles

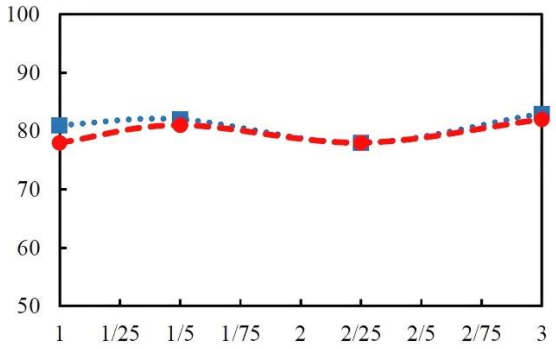

Figure 18: Pile head efficiency for different spacing ratios of two-blade and three-blade screw piles

The maximum settlement of the underlying soil is shown in Figure (19). The results indicate that the lowest settlement is obtained for the two-blade pile with a spacing ratio of 1.5 and the three-blade pile with a spacing ratio of 3, which is equal to the settlement of the single-blade screw pile. From the results obtained, it can be concluded that due to the frictional behavior of the pile, the pile body wall plays an important role in controlling the settlement rate in a pile-based embankment system, and adding a pile blade has no effect on controlling the settlement rate in the overall performance of the system and may even make the situation critical.

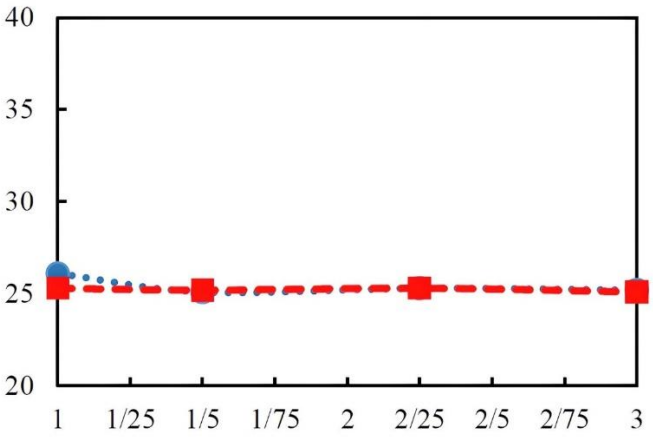

Figure 19: Subsoil settlement for different spacing ratios of two-blade and three-blade screw piles

Conclusion

Abaqus was used to finite element assess screw and solid concrete pile embankments and total heck's effect on screw piles. After verifying the results of the numerical model on an embankment based on concrete piles and the load-settlement model of screw piles, the difference between screw and concrete piles on the performance of the system under the same loading conditions and soil engineering parameters was investigated. The most important results of the present study include the following:

1- Screw piles handle embankment and foundation settling better than concrete piles because the center settles 10% less and decreases with distance.

2- The stress reduction ratio in this research reveals that concrete piles create the embankment load transfer mechanism better than tubular screw pile shafts owing to their more significant cross-sectional area.

3- Improving load transfer does not affect the embankment system's horizontal and vertical settlements.

4- The height of the embankment promotes weight transfer and decreases change.

5- Screw pile caps spread force. Caps reduce vertical settling by 19% due to more excellent pile stress transfer and foundation soil pressure reduction.

6- A blade on the pile body enhances load transfer but does not screw pile embankments at a 1.5 distance.

References

1. Kassou, F., et al., *Slope stability of embankments on soft soil improved with vertical drains.* Civil Engineering Journal, 2020. **6**(1): p. 164-173.
2. Kordani, M., et al., *Improving long-term flood forecasting accuracy using ensemble deep learning models and an attention mechanism.* Journal of Hydrologic Engineering, 2024. **29**(6): p. 04024042.
3. Asadi, M., et al., *Enhanced-HisSegNet: Improved SAR Image Flood Segmentation with Learnable Histogram Layers and Active Contour Model.* IEEE Geoscience and Remote Sensing Letters, 2025.
4. Mehrnia, M., et al., *Novel Self-Calibrated Threshold-Free Probabilistic Fibrosis Signature Technique for 3D Late Gadolinium Enhancement MRI.* IEEE Transactions on Biomedical Engineering, 2024.
5. Sharafkhani, F., S. Corns, and R. Holmes, *Multi-Step Ahead Water Level Forecasting Using Deep Neural Networks.* Water, 2024. **16**(21): p. 3153.
6. Wang, K., et al., *The soil-arching effect in pile-supported embankments: A review.* Buildings, 2024. **14**(1): p. 126.
7. Hajrasouliha, A. and B.S. Ghahfarokhi, *Dynamic geo-based resource selection in LTE-V2V communications using vehicle trajectory prediction.* Computer Communications, 2021. **177**: p. 239-254.
8. Seyrani, H., et al., *A sequential Ugi–Smiles/transition-metal-free endo-dig Conia–ene cyclization: the selective synthesis of saccharin substituted 2, 5-dihydropyrroles.* New Journal of Chemistry, 2021. **45**(34): p. 15647-15654.
9. Deng, Y., et al., *Research on static and dynamic loading performance of geosynthetic reinforced and pile-supported embankment.* Applied Sciences, 2023. **13**(24): p. 13152.
10. Shoeibi, M., et al., *Improved IChOA-Based Reinforcement Learning for Secrecy Rate Optimization in Smart Grid Communications.* Computers, Materials & Continua, 2024. **81**(2).
11. Khatami, S.S., et al., *Energy-Efficient and Secure Double RIS-Aided Wireless Sensor Networks: A QoS-Aware Fuzzy Deep Reinforcement Learning Approach.* Journal of Sensor and Actuator Networks, 2025. **14**(1): p. 18.
12. Khatami, S.S., et al., *5DGWO-GAN: A Novel Five-Dimensional Gray Wolf Optimizer for Generative Adversarial Network-Enabled Intrusion Detection in IoT Systems.* Computers, Materials & Continua, 2025. **82**(1).

13. Zhao, J. and J. Zhang. *Parametric analysis of geosynthetic reinforced and pile supported embankment*. in *2015 International Conference on Mechatronics, Electronic, Industrial and Control Engineering (MEIC-15)*. 2015. Atlantis Press.
14. Su, Q. and J. Huang, *Deformation and failure modes of composite foundation with sub-embankment plain concrete piles.* Sciences, 2013. **5**.
15. Zhang, Z., et al. *Numerical analysis of geosynthetic-reinforced pile-supported embankments subjected to different surface loads*. in *Geo-Congress 2020*. 2020. American Society of Civil Engineers Reston, VA.
16. Umravia, N. and C. Solanki. *Comparative study of existing cement fly ash gravel pile and encased stone column composite foundation*. in *IOP Conference Series: Materials Science and Engineering*. 2021. IOP Publishing.
17. Fariman, S.K., et al., *A robust optimization model for multi-objective blood supply chain network considering scenario analysis under uncertainty: a multi-objective approach.* Scientific Reports, 2024. **14**(1): p. 9452.
18. Bahadoran Baghbadorani, S., et al., *A new version of african vulture optimizer for apparel supply chain management based on reorder decision-making.* Sustainability, 2022. **15**(1): p. 400.
19. Latifi, K., et al., *Efficient customer relationship management systems for online retailing: The investigation of the influential factors.* Journal of Management & Organization, 2023. **29**(4): p. 763-798.
20. Umravia, N. and C. Solanki, *Numerical analysis to study lateral behavior of cement fly ash gravel piles under the soft soil.* Int. J. Eng, 2022. **35**: p. 2111-2119.
21. Lv, G.-h., et al., *Experimental Study on Embankment Failure Law and Reinforcement Technology for Highway Widening Project over Silt Soils.* Journal of Testing and Evaluation, 2021. **49**(6): p. 4248-4260.
22. Chen, R.P., et al., *Field tests on pile-supported embankments over soft ground.* Journal of Geotechnical and Geoenvironmental Engineering, 2010. **136**(6): p. 777-785.
23. Lashaki, R.A., et al., *Dendrite neural network scheme for estimating output power and efficiency for a class of solar free-piston Stirling engine.* International Journal of Modelling and Simulation, 2025: p. 1-12.
24. Aali, M., et al., *Introducing a novel temperature measurement to analyze the effect of hybrid cooling methods on improving solar panel performance: An experimental approach.* Applied Thermal Engineering, 2025: p. 125889.
25. Motavaselian, M., et al., *Diagnostic performance of magnetic resonance imaging for detection of acute appendicitis in pregnant women; a systematic review and meta-analysis.* Archives of academic emergency medicine, 2022. **10**(1): p. e81.
26. Davidson, C., et al., *Centrifuge modelling of screw piles for offshore wind energy foundations*, in *Physical Modelling in Geotechnics, Volume 1*. 2018, CRC Press. p. 696-700.
27. Abbas, H.O. and O.K. Ali. *Parameters affecting screw pile capacity embedded in soft clay overlaying dense sandy soil*. in *IOP Conference Series: Materials Science and Engineering*. 2020. IOP Publishing.
28. Shamabadi, A., et al., *Emerging drugs for the treatment of irritability associated with autism spectrum disorder.* Expert Opinion on Emerging Drugs, 2024. **29**(1): p. 45-56.
29. Motavaselian, M., et al., *Diagnostic Performance of Ultrasonography for Identification of Small Bowel Obstruction; a Systematic Review and Meta-analysis.* Archives of Academic Emergency Medicine, 2024. **12**(1): p. e33.
30. Abdelghany, Y. and M.H. El Naggar, *Full-scale field investigations and numerical analyses of innovative seismic composite fiber-reinforced polymer and reinforced grouted helical screw instrumented piles under axial and lateral monotonic and cyclic loadings*, in *Advances in soil dynamics and foundation engineering*. 2014. p. 414-424.
31. Bagheri, F. and M. El Naggar, *Effects of installation disturbance on behavior of multi-helix piles in structured clays.* DFI Journal-The Journal of the Deep Foundations Institute, 2015. **9**(2): p. 80-91.
32. Abd El Raouf, M.E., *Finite Element Analysis of Embankments on Soft Clay.* Journal of Al-Azhar University Engineering Sector, 2020. **15**(57): p. 963-970.

33. Fan, C., et al., *Poisson's ratio of granular materials for Mohr-Coulomb elastoplastic model.* International Journal of Mining, Reclamation and Environment, 2023. **37**(10): p. 780-804.
34. Jung, J.K., T.D. O'Rourke, and N.A. Olson, *Lateral soil-pipe interaction in dry and partially saturated sand.* Journal of geotechnical and geoenvironmental engineering, 2013. **139**(12): p. 2028-2036.
35. Tepho, T., et al. *Development of a traffic load model for bridge structures within an urban subway system*. in *IABSE Congress Ghent 2021-Structural Engineering for Future Societal Needs*. 2021.
36. Goicolea, J.M., F. Gabaldón, and F. Riquelme, *Design issues for dynamics of high speed railway bridges.* International Association for Bridge Maintenance and Safety, Porto, 2006.
37. Al-Karawi, H., P. Shams-Hakimi, and M. Al-Emrani, *Mean stress effect in high-frequency mechanical impact (HFMI)-treated steel road bridges.* Buildings, 2022. **12**(5): p. 545.
38. Xu, C., S. Song, and J. Han, *Scaled model tests on influence factors of full geosynthetic-reinforced pile-supported embankments.* Geosynthetics International, 2016. **23**(2): p. 140-153.